JOC The Journal of Organic Chemistry

Article

pubs.acs.org/joc

Insight into the Isoelectronic Character of Azomethines and Vinylenes Using Representative Models: A Spectroscopic and Electrochemical Study

Andréanne Bolduc,[†] Abelaziz Al Ouahabi,[†,‡] Charlotte Mallet,[†,§] and W. G. Skene*[,†]

[†]Laboratoire de caractérisation photophysique des matériaux conjugués, Département de Chimie, Université de Montréal, CP 6128, Centre-ville Montreal, QC H3C 3J7, Canada

[‡]Institut Charles Sadron (UPR22-CNRS) 23 rue du Loess, BP 84047, 67034 Strasbourg Cedex 2, France

[§]Department of Polymer Science and Engineering, University of Massachusetts - Amherst, Conte center for polymer research, 120 Governors Drive, Amherst, Massachusetts 01003, United States

Supporting Information

ABSTRACT: A series of azomethine and vinylene dyad and triad analogues were prepared. Their absorbance, fluorescence, and redox properties were examined experimentally and theoretically using density functional theory (DFT) calculations. These measurements were done to determine the effect of the heteroatom of the azomethine relative to its all-carbon counterpart and to assess the isoelectronic character of the two bonds. The orientation of the azomethine was found to have little effect on the absorbance, fluorescence, and electrochemical properties. In contrast, the spectral and electrochemical properties were highly contingent on the electronic groups and degree of conjugation. The spectral properties could be tuned 200 nm across the visible region. More importantly, the heteroatom in the conjugated bond was found to give rise to only a 20 nm bathochromic shift in the absorbance and fluorescence spectra. The fluorescence quantum yield (Φ_{Fl}) of the vinylene derivatives varied between 5% and 20% with fluorescence quenching occurring by photoisomerization from the *E* to *Z* isomers. In contrast, the fluorescence of the analogous azomethine derivatives was completely quenched. The collective spectroscopic and electrochemical ab initio DFT data additionally confirmed that the azomethine and its analogous vinylene are isoelectronic. It was also found that a conjugated thiophene vinylene dyad with primary amines in the α,α'-positions could be prepared and isolated. The compound was stable under aerobic conditions providing electron withdrawing (either ester or nitrile) groups were located in the adjacent positions.

INTRODUCTION

Conjugated materials have received much attention, owing to their optoelectronic properties that are suitable for plastic electronic applications.[1−4] Thiophenes have been the choice building block for preparing such materials. This is in part due to their low oxidation potentials that are ideal for both chemical and electrochemical synthesis of highly conjugated compounds. Despite this advantage, the chemical synthesis of conjugated thiophenes involving carbon−carbon coupling requires stringent reactions such as Suzuki coupling,[5] Stille coupling[6,7] and Heck coupling,[8] to name but a few. The synthesis of donor−acceptor conjugated materials is additionally challenging because of reactivity incompatibilities between reagents and catalysts that lead to low yields and unselective product formation. Therefore, methods for preparing donor−acceptor conjugated materials that have desired optoelectronic properties are of interest.[9,10]

We recently addressed this challenge by using azomethines (−N═CH−) as functional materials. The advantage of the heteroatomic materials over their vinylene counterparts is the ease of preparation. Azomethines are prepared by the straightforward condensation of complementary amines and aldehydes. The reaction can be done using mild conditions at room temperature with catalytic mineral acids.[11,12] The products can further be purified by straightforward precipitation. Azomethines are additionally interesting as functional materials because of the inherent electron-withdrawing property of the heteroatomic bond. When coupled to electron rich heterocycles, this results in highly conjugated π-donor−acceptor materials. These compounds can have optoelectronic properties that are of interest for use in device applications and that are comparable to their all-carbon counterparts.

Azomethines are commonly accepted as being isoelectronic to their all-carbon counterparts.[13] There are nonetheless differences in their properties, notably their photostability, fluorescence, and redox potentials.[14] Extensive structure−property studies have subsequently been undertaken for optimizing the optoelectronic properties of azomethines.[11] Despite these studies, there is still little known about the collective effect of the azomethine bond and various electronic groups on the optoelectronic properties. This is in part owing to the limited number of stable aminothiophenes available for preparing conjugated azomethines. As a result, the stable 2,5-

Received: July 10, 2013
Published: August 15, 2013

   dx.doi.org/10.1021/jo401497z | J. Org. Chem. 2013, 78, 9258−9269

diamine (**1**; Chart 1) has predominately been used for preparing conjugated azomethines that are stable under ambient aerobic conditions. The stability of **1** and its azomethine products are courtesy of the stabilizing effect of the esters in the 3 and 4 positions.

Their synthetic and purification advantages concomitant with their isoelectronic character make azomethines interesting replacements for their all-carbon counterparts. The successful use of vinyl derivatives in plastic electronics such as organic photovoltaics[15,16] and organic light emitting diodes,[17,18] would suggest that azomethines would also be suitable for such applications. It is therefore important to understand the effect of the various electronic groups on the optoelectronic properties for designing and preparing azomethines with enhanced properties relative to their analogous vinyl derivatives. Most importantly, the effect of the nitrogen atom in the azomethine and stabilizing esters are of importance for comparing the properties among similar compounds. For this reason, we prepared the previously unreported and air-stable 2-aminothiophene vinylene **4**, whose synthesis, spectroscopy, and electrochemistry are herein presented. The effect of the esters and the azomethine nitrogen on the spectroscopic and electrochemical properties is further examined by comparing to the analogous compounds in Chart 1. The spectroscopic properties and energy levels of 2-aminothiophene derivatives that could not be synthesized were additionally calculated theoretically. The collective experimental and theoretical data were compared for understanding the structural modifications and electronic effects on the spectroscopic and electrochemical properties of conjugated oligomers.

Chart 1. Vinylene and Azomethine Analogues Investigated

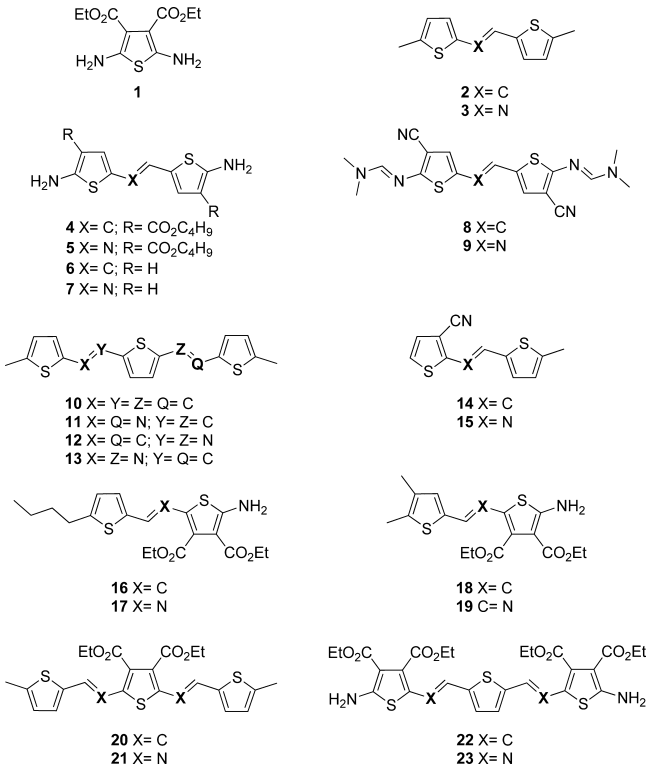

RESULTS/DISCUSSION

Synthesis. The ester-free derivative (**7**) would be an ideal model compound for direct comparison of the physical properties to both the vinylene analogue (**2**) and the azomethines in Chart 1. However, it could not be isolated and it spontaneously decomposed. For this reason, **4** was targeted. It was surmised that the electron withdrawing ester in the 3-position would stabilize the targeted product, similar to its unsubstituted counterpart 2-aminothiophene.[19−21]

The synthesis of **4** was done according to the synthetic scheme outlined in Scheme 1. This involved preparing the activated ester **4a** according to known means in high yields.[22] It was then reacted with 1,4-dithiane-2,5-diol via the Gewald reaction under basic conditions to afford the air-stable 2-

Scheme 1. Synthetic Scheme for the Preparation of 4: (i) 80 °C, 16 h; (ii) 45 °C, DMF; (iii) rt 16 h, CH_2Cl_2; (iv) 60 °C, 16 h, Dioxane; (v) $TiCl_4/ZnCl_2$, THF

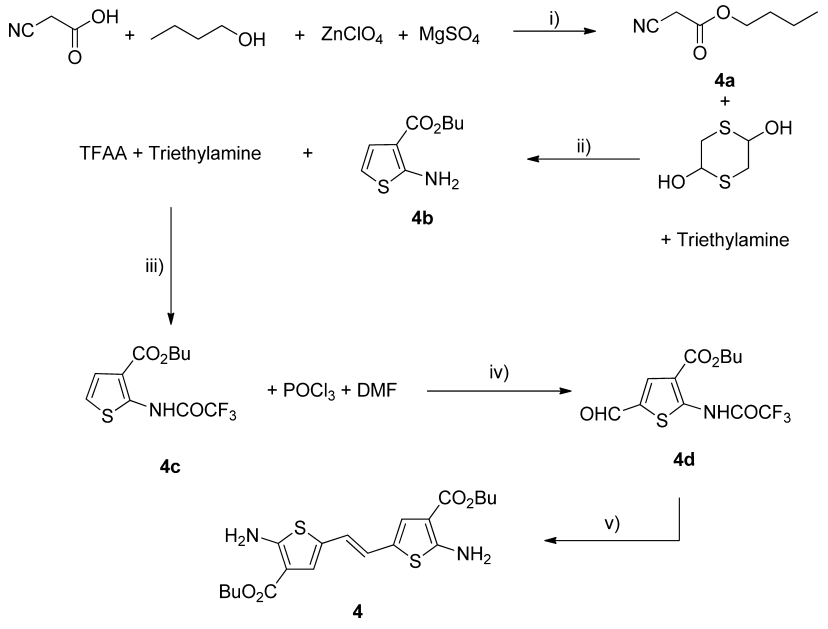

dx.doi.org/10.1021/jo401497z | J. Org. Chem. 2013, 78, 9258−9269

Scheme 2. Synthetic Scheme for the Preparation of 8: (i) $POCl_3$, 60 °C, DMF; (ii) $TiCl_4/ZnCl_2$, THF

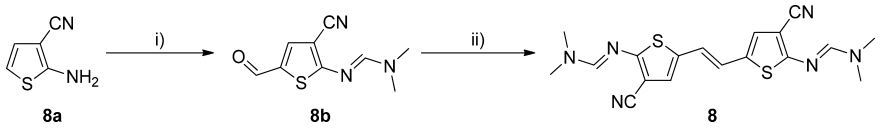

aminothiophene **4b**.[23] Although the product is inert, the amine group is still reactive, especially under Vilsmeier−Haack and McMurry reaction conditions. **4b** was subsequently protected as an amide with trifluoroacetic anhydride, which was confirmed by both ^{1}H and ^{19}F NMR. The protection was extremely sluggish, unlike that for protecting **4b** with ^{t}BOC. The latter was originally chosen, but the protecting group did not withstand the McMurry coupling conditions. The desired aldehyde was incorporated into **4c** via Vilsmeier−Haack formylation. The isolated **4d** was then subjected to McMurry coupling. Formation of the desired vinylene was found to occur only when zinc was added to a $TiCl_4$ solution in tetrahydrofuran (THF) and allowing it to stir for 30 min before adding **4d**. The resulting product was found to be unstable. It was subsequently deprotected with potassium carbonate without isolating it beforehand. The reactions were additionally done in the dark to prevent photoisomerization of the vinylene products. Although the *E* isomer of **4** was predominately formed, it could be isolated from the undesired *Z* isomer by column chromatography. The targeted **4** was isolated as a yellow solid. Although the product could be isolated and handled under ambient conditions, it was photochemically unstable, requiring protection against ambient light when stored.

Compound **8** was also targeted. This was because the azomethine formed from the dimethylformamidine (DMF) protecting group has a limited degree of conjugation relative to conjugated azomethines such as **11**, **13**, and **21**. Therefore, the effect of the azomethine bond on the photophysical and electrochemical properties relative to conjugated azomethines can be examined. The targeted **8** was prepared similarly to **4** but starting from **8a** (Scheme 2). **8a** was formylated directly, and it was protected in situ by DMF. The protecting group was expected to be removed with conditions similar to those of **4**. In contrast, only the protected product was obtained. Multiple attempts to deprotect **8** were unsuccessful with known methods, including hydrochloric acid and trifluoroacetic acid. The electron withdrawing differences of the nitrile and ester groups are most likely responsible for the different stability of the protecting group.

The syntheses of **10**, **21**, and **23** were done according to previously described methods.[24,25] The azomethine derivatives **15**, **17**, and **19** were prepared from the corresponding amine and aldehyde in a 1:1 ratio in ethanol along with a catalytic amount of trifluoroacetic acid. The reaction mixture was then stirred overnight at room temperature. No inert atmosphere or anhydrous solvents were required. In the case of **15**, the resulting dimer was insoluble in ethanol, and the product precipitated overnight. The desired product was obtained pure in a considerable yield by filtering the solution and washing it with cold ethanol. In contrast, **17** and **19** required additional purifications to isolate them from the undesired trimers that were formed as byproducts. Purification by flash column chromatography was thus performed and the compounds were obtained in moderate yield. Differences in yields were observed for **17** (20%) and **19** (75%) owing to the instability of the 5-butylthiophene-2-carboxaldehyde starting material. The yields are nonetheless consistent with those of **4** and **8**. The low overall yields for the aminothiophene vinylenes are a result of the stringent reactions, multistep preparation, and mixture of *E* and *Z* isomers.

The vinylene model compound (**2**) was prepared according to standard McMurry coupling procedures.[26] No extensive purification was required for the compound. The desired *E* isomer was isolated by recrystallization in carbon tetrachloride, as confirmed by ^{1}H NMR.

X-ray Structure. Monocrystals of **8** suitable for X-ray diffraction (XRD) analyses were grown from the slow evaporation of acetone. These crystals were grown to see whether the resulting compound was coplanar similar to analogous azomethines.[27] XRD further provides unequivocal confirmation that the *E* isomer of the unsaturated bond was obtained, as was confirmed by ^{1}H NMR. As shown in Figure 1,

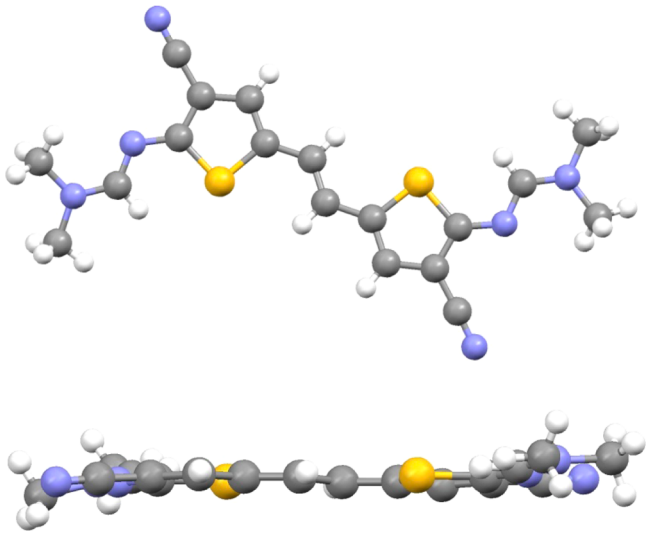

Figure 1. Face (top) and edge (bottom) views of the resolved XRD crystal structure of **8**.

8 is highly coplanar with a mean plane torsion angle between the two thiophene rings of 1.96(1)°. The high degree of coplanarity adopted by the thiophenes with respect to the vinylene is evident in the face and edge views of Figure 1. The configuration adopted is similar to that of corresponding azomethines.[27]

8 organized itself in a *zigzag* packing in the crystal lattice (Figure 2) and it crystallized in the orthorhombic *Pbca* space group. Its organization is driven mostly by hydrogen bonding between the cyano group and the adjacent hydrogens as shown in top of Figure 3. Two different hydrogen bonding motifs were found in the crystal packing. Bonding between the cyano groups and hydrogen from the methyl terminal group was found at a distance of 2.647(1) Å. The short distance is common for H-bonding.[28] This is assumed to lead to the *zigzag* configuration, because the molecules organize themselves at

dx.doi.org/10.1021/jo401497z | J. Org. Chem. 2013, 78, 9258−9269

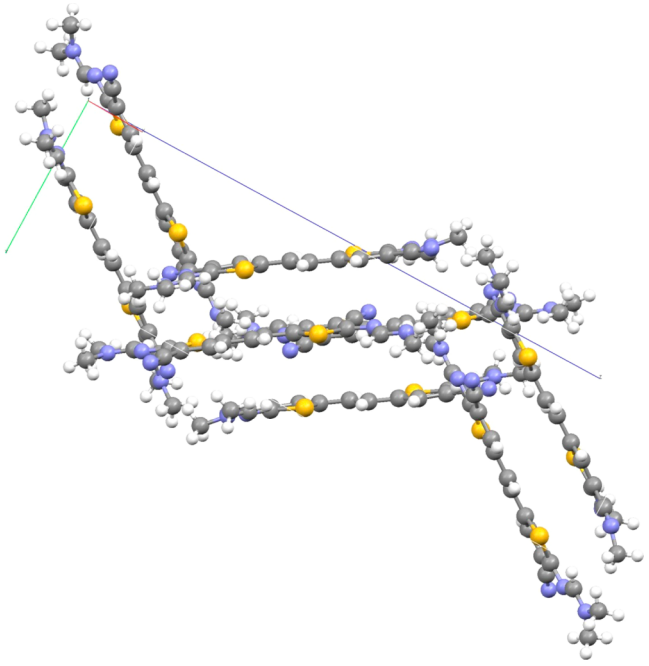

Figure 2. Crystal lattice packing of **8**.

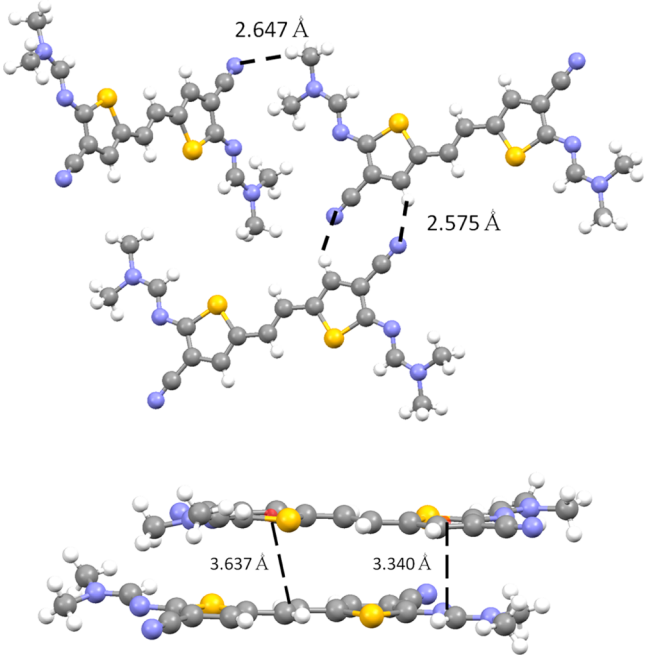

Figure 3. Intramolecular hydrogen bonding (top) and π-stacking (bottom) found in the crystal lattice of **8**.

68.6(1)° from each other. The molecules also organize themselves on the same plane via cyano−hydrogen interactions. The cyano groups also hydrogen bond at 2.575(1) Å with the adjacent thiophene.

The molecular organization in the lattice is also driven by various intermolecular π-stacking interactions. One occurs between the thiophene's centroid and the vinyl bond and another takes place between the remaining thiophene's centroid and the azomethine bond of the dimethylformamide protecting group. These interactions occur respectively at distances of 3.637(1) and 3.340(1) Å and they are within the acceptable range for $\pi-\pi$ stacking.[29] Interestingly, a similar packing behavior was observed in azomethines, where the thiophene centroid had π interactions with the azomethine between thiophenes.[30]

Photophysical Properties. The photophysical properties of the azomethines and vinylene analogues from Chart 1 were investigated. Notably, the absorbance, fluorescence, and fluorescence quantum yields of these compounds were measured to assess the structural and electronic effects on the spectroscopic properties. These effects can be assigned by comparing the spectroscopic properties of the different compounds. For example, the impact of the degree of conjugation can be seen by comparing **2**, **4**, **8**, and **10** as well as azomethine derivatives **15**, **17**, **18**, **21**, and **23**. The effects of the azomethine bond, amine electron donating, and ester withdrawing groups can be assigned by comparing both **21** and **23** to **10**. The electronic effects can similarly be evaluated from comparing **2**, **4**, and **8**. Meanwhile, the electron donating and withdrawing effects can be evaluated by comparing the spectral properties of **2**, **4**, **15**, **17**, and **19**.

As can be seen by the collective absorbance spectra in Figure 4 and the data in Table 1, the absorbance can be tailored

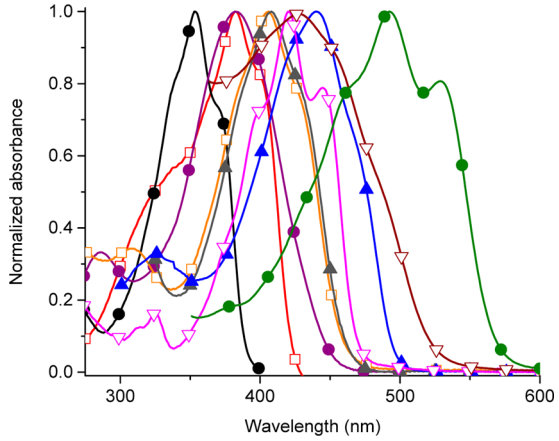

Figure 4. Normalized absorbance of **2** (black ●), **4** (red □), **8** (blue ▲), **10** (red ▽), **15** (purple ●), **17** (orange □), **19** (green ▲), **21** (brown ▽), and **23** (green ●) measured in dichloromethane.

approximately 200 nm across the visible region with subtle structural modifications and with electronic groups. For example, an 87 nm red shift in the absorbance occurs as a

Table 1. Photophysical Properties of the Compounds Measured in Deaerated Dichloromethane

compound	λ_{abs} (nm)	λ_{em} (nm)	Φ_{fl} (%)[a]	ΔE (eV)[b]	$E_{g\ spectro}$ (eV)[c]
2	353	412	5	3.2	3.1
4	382	500	7	2.8	2.7
8	440	497	20	2.6	2.5
10	445	498	15	2.7	2.6
15	382	468	≈0	3.0	2.7
17	406	500	≈0	2.8	2.6
19	408	497	≈0	2.8	2.6
21[e]	427	459	≈0	2.5	2.2
23[e]	493	594	≈ 0	2.2	2.1

[a]Absolute quantum yield measured with an integrating sphere. [b]Absolute energy gap taken from the intercept of the normalized absorbance and fluorescence spectra. [c]Spectroscopically derived energy-gap. [d]From the literature.[25] [e]From the literature.[12]

dx.doi.org/10.1021/jo401497z | J. Org. Chem. 2013, 78, 9258−9269

result of increasing the degree of conjugation from **2** (353 nm) to **10** (445 nm). A similar red shift of 45 nm is also observed between **15** and **21** as a result of the increased degree of conjugation. However, the observed red shift cannot be assigned uniquely to the increase in conjugation, given the different electron withdrawing groups of **15** and **21**. The stronger electron withdrawing character of the cyano group affects the optoelectronic properties (vide supra). The additional thiophene in **15**–**21** is also in part responsible of the observed red shift. Meanwhile, the 66 nm bathochromic shift of **23** relative to that of **21** is owing to the electron donating effect of the terminal amines. These two compounds can be directly compared because the orientation of the azomethine does not effect the HOMO and LUMO levels (see Figure 9 and Table 3). The effect of the terminal amines is further seen when comparing **2** with **4**, whose absorbance difference is 30 nm. The shift between **2** (353 nm) and **4** (382 nm) is less than that for **21** (427 nm) and **23** (493 nm) owing to the different number of ester withdrawing groups. The electronic *push*–*pull* effect resulting from the amine/azomethine is further seen by the 58 nm bathochromic shift of **8** relative to **4**.[27] This effect is highly noticeable from the absorbance maximum that is red-shifted by 90 nm relative to that of **2**. Of particular interest is the effect of the heteroatom in the azomethine on the spectroscopic properties. Although the unique effect of the azomethine on the spectral properties cannot unequivocally be assessed relative to its all-carbon counterpart, **2** and **15** are the best representative models for such a comparison. The weak donating effect of the 2,2′-methyl groups of **2** accounts for a red shift of 2 nm, according to the spectral shifts observed for **17** (406 nm) and **19** (408 nm). The azomethine therefore gives rise to a 27 nm bathochromic shift. Although large spectral differences were not observed between the all-carbon bond and azomethine counterparts, the heteroatomic bond nonetheless results in red-shifted spectra. Enhanced spectral shifts are possible by taking advantage of the electronic effect of the azomethine by conjugating it with electron rich and/or electron donating groups. The resulting electronic *push*–*pull* systems absorb in the visible such as **21** and **23**.[11,27]

The same trend in absorbance shifts as a function of structure was also observed for the fluorescence of the compounds examined. The exceptions to the trend were **4** (382 nm) and **21** (427 nm) that were red and blue shifted, respectively, from what was expected. Although the exact reason for these exceptions is not known, there was a significant difference in the fluorescence quantum yields (Φ_{fl}) for the compounds. As seen in Table 1, the azomethines essentially do not fluoresce. To some extent, this is not surprising because the heteroatomic bond is known to rapidly deactivate the singlet excited state by photoinduced electron transfer.[31] The excited state is additionally known to be efficiently deactivated by internal conversion involving bond rotation.[32] In the case of thiophene azomethine derivatives, intersystem crossing to the triplet state is also an efficient deactivation mode.[33] The collective deactivation modes ensure the quenched fluorescence of azomethines such that the Φ_{fl} is below what can be accurately measured by an integrating sphere (<2%).

In contrast to the azomethines, the vinylene derivatives fluoresced in appreciable amounts (5–20%), and these could be measured accurately with an integrating sphere. The measured values were well below unity, which is not surprising because oligothiophenes are known to efficiently intersystem cross (vide supra).[34−36] The triplet formed by this process can be spectroscopically detected by laser flash photolysis. This technique was subsequently used to determine the presence of triplets. No triplet transient was detected either for **2** or **4**. The intense laser pulse at 355 nm led exclusively to a photoproduct having a much longer lifetime than the resolution of the instrument (>100 μs). The long lifetime precludes a triplet transient given they typically have unimolecular lifetimes <100 μs.[37] To further identify the photoproduct, **2** was irradiated at 350 nm under steady-state conditions. As seen in Figure 5, the

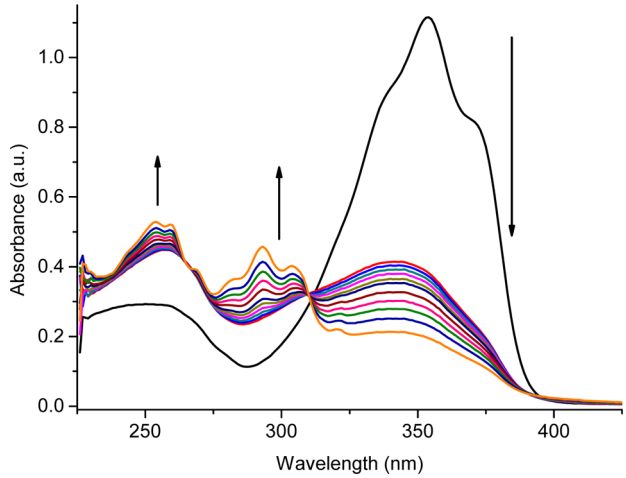

Figure 5. Change in absorbance spectra of **2** when irradiated at 350 nm between 0 (black) and 170 min (orange) in deaerated and deuterated chloroform.

original absorbance spectra **2** (λ_{max} = 350 nm) are converted into a spectrum whose absorbance is shifted to 295 nm. The blue shift in the photoproduct absorbance suggests it has a decreased degree of conjugation relative to **2**. Meanwhile, the isosbestic point at 310 nm confirms the presence of only two species that are interdependent. The photoproduct was subsequently analyzed by ^{1}H NMR and it was found to be the cis isomer. The low Φ_{fl} observed for **2** therefore is from trans → cis photoisomerization and not singlet excited state quenching by intersystem crossing. The vinylene compounds are therefore photounstable. This is in contrast to their azomethine counterparts that are photostable and do not photoisomerize even at prolonged irradiated times.[38]

Electrochemical Properties. The electrochemical properties of the compounds were also examined by cyclic voltammetry to determine the oxidation and reduction potentials of the compounds. This was done to accurately assess the structure–property relationships and correlate the electrochemical properties with the spectroscopic properties. The reduction process was irreversible for all the compounds investigated. In contrast, the oxidation process was reversible for all compounds except for **15**. Electrochemical reversibility was quantitatively confirmed from the equal peak current of the forward and reverse scans.[39] The oxidation process was found to be a one-electron, according to known means.[40] Meanwhile, the formal oxidation potential (E^o) was calculated from the forward and reverse oxidation potentials.

Cyclic voltammetric measurements were done at various scan rates to further confirm quantitatively the oxidation reversibility, type of process (reversible, quasi-reversible, and pseudo-reversible), and number of electrons transferred in the

dx.doi.org/10.1021/jo401497z | J. Org. Chem. 2013, 78, 9258–9269

oxidation. The number of electrons (n) involved in the oxidation was quantified by comparing the peak currents of ferrocene to the given sample for the forward scans, according to the Randles–Sevcik equation:[41]

$$i = (2.69 \times 10^5)n^{3/2}AD^{1/2}Cv^{1/2}$$

where i is the anodic peak current, n the number of electrons transferred, A the working electrode area, D the diffusion coefficient, C the concentration, and v the scan rate. The equation simplifies to

$$i = n^{3/2}v^{1/2} \times \text{constant}$$

when equimolar ferrocene is used as the internal reference. The desired n can be determined by plotting the anodic peak current as a function of scan rate (Figure 6). Because the oxidation of ferrocene is a one-electron process, the ratio of the slopes (Figure 6) gives the desired n.[42] According to this means, all the compounds, except **15**, were found to reversibly undergo a one-electron oxidation, resulting in the radical cation. The reversible oxidation observed confirms that the resulting radical cation is stable and that it does not couple according to standard anodic means.[43]

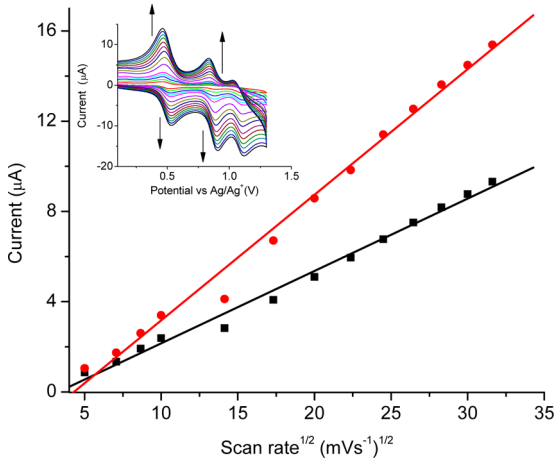

Figure 6. Current as a function of scan rate for **10** (■) and ferrocene (●). Inset: anodic cyclic voltammograms of **10** measured at 10 (black), 25 (red), 50 (green), 75 (blue), 100 (light blue), 200 (pink), 300 (yellow), 400 (tan), 500 (gray), 600 (purple), 700 (brown), 800 (dark green), 900 (teal), and 100 (dark blue) mV s^{-1} with 0.1 M tetrabutylammonium hexafluorophosphate ($TBAPF_6$) in anhydrous and deaerated dichloromethane.

The forward scan ($E_{forward}$) oxidation potentials for the various compounds were used to examine the effect of structure and electronic effects on the potentials. The typically used E_{pa} could not be applied for comparing the potentials of the different compounds because of the irreversible oxidation of **15**. $E_{forward}$ is independent of the oxidation reversibility making for accurate assessment of the oxidation potential contingent on structure. The oxidation onset was additionally used to calculate the HOMO energy level. This was done according to the commonly accepted approximation: HOMO = $-e(E_{pa}^{onset} + 4.72)$, where the potentials are measured against Ag/Ag$^+$,[44−47] and by taking the E' of the internal reference ferrocene as 0.35 V vs Ag/AgCl.[48] Similarly, the LUMO energy level was calculated according to LUMO = $-e(E_{pc}^{onset} + 4.72)$. The approximations are valid if the redox processes form radical ions. Given the reduction process of the compounds cannot be unequivocaly assigned, the LUMO energy levels cannot be accurately evaluated electrochemically. Nonetheless, the collective electrochemical data for the compounds from Chart 1 are summarized in Table 2 and representative anodic cyclic voltammograms are found in Figure 7.

Table 2. Electrochemical Properties of Compounds from Chart 1 Measured in Deaerated Dichloromethane[a]

compound	$E_{forward}$ (E^0) (V)[b]	HOMO (eV)	LUMO (eV)	$E_{g\ electro}$ (eV)
2	1.09 (1.02)	−5.4	−3.2	2.2
4	0.54 (0.51)	−4.8	−3.0	1.8
8	0.65 (0.63)	−5.0	−2.9	2.1
10	0.82 (0.80)	−5.1	−3.4	1.7
15	1.65 (−)	−6.0	−2.9	3.1
17	0.88 (0.85)	−5.2	−2.9	2.3
19	0.89 (0.86)	−5.2	−2.9	2.3
21[c]	0.86 (0.83)	−5.2	−3.0	2.2
23[d]	0.87 (0.82)	−5.2	−3.1	2.1

[a]Measured against Ag/Ag$^+$. [b]$E_{forward}$ refers to the oxidation potential for the forward scan. Value in parentheses refers to formal potential determined from the reversible oxidation couple. [c]From the literature.[25] [d]From the literature.[12]

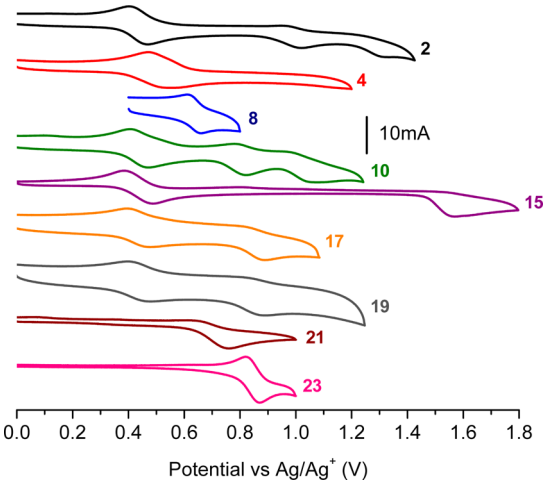

Figure 7. Anodic cyclic voltammograms of **2** (black), **4** (red), **8** (blue), **10** (green), **15** (purple), **17** (orange), **19** (gray), **21** (brown), and **23** (pink) vs Ag/Ag$^+$ with 0.1 M $TBAPF_6$ in anhydrous and deaerated dichloromethane with ferrocene as an internal reference. Ferrocene was not added to **4** and **8** because of overlapping oxidation potentials.

It is evident from the electrochemical data that the vinyl derivatives have lower oxidation potentials than their azomethine analogues. This is obvious upon comparing **2** whose oxidation potential is 560 mV less positive than that of **15**. Similarly, the oxidation potentials of **17** and **19** are 360 mV more positive than the analogous **4**. The more positive potentials observed for the azomethines relative to the all-carbon counterparts can be ascribed to the electron withdrawing effect of the heteroatomic bond. Interestingly, **4** (540 mV) had the lowest oxidation potential of the compounds examined, owing to the electron donating amines. The measured value of **4** was more positive than the reduction potential of oxygen, confirming its observed stability under ambient conditions. The effect of degree of conjugation and electronic effects on the oxidation potential are consistent with the spectroscopic data. For example, E_{pa} of **10** is 20 mV lower

dx.doi.org/10.1021/jo401497z | J. Org. Chem. 2013, 78, 9258−9269

than that of **2**, owing to the increased degree of conjugation. Meanwhile, the E_{pa} of **4** is 10 mV lower than that of **8** as a result of the amine electron donating effect as opposed to the withdrawing azomethine character. While **10** (820 mV), **17** (880 mV), **21** (860 mV), and **23** (870 mV) are structurally different, they have similar E_{pa}. This is owing to the collective electronic effects and degree of conjugation.

Theoretical Calculations. Given the synthetic challenges in isolating aminothiophene vinylene derivatives such as **11** and **13** for analyzing their spectroscopic and electrochemical properties, the desired properties were empirically calculated. This method was chosen to accurately evaluate the effect of the azomethine on the optoelectronic properties without the electron withdrawing ester/nitrile group, which is otherwise required for synthetically preparing the compounds. The properties were calculated using DFT and 6-31G* basis sets. The geometries were first optimized semi-empirically using Austin model 1 (AM1) followed by single point energy calculations with DFT. This approach was selected because of the shorter AM1 geometry optimization computation times without sacrificing accuracy. The latter was confirmed by comparing the bond lengths and energies of optimized geometries for a model **8** calculated semi-empirically and by DFT. Both methods gave similar results. Moreover, the calculated bond angles and lengths for the AM1 calculations correlated better with X-ray diffraction data. The properties of the synthesized compounds from Chart 1 were first calculated. These were used as a benchmark to verify the empirically calculated values against the experimentally measured properties. Although absolute values cannot be precisely calculated empirically, relative values, however, can be accurately measured within a given series. Figure 8 shows a comparison of the experimental and theoretical data. The calculated and measured HOMO energy levels are similar. This is not surprising because the B3LYP 6-31G* basis set is known to accurately estimate the HOMO energy levels of conjugated materials.[49,50] This is in contrast to the LUMO energy values that cannot be as accurately calculated. This, in part, accounts for the calculated LUMO energy levels being less negative than the experimentally measured values. However, it was shown that the B3LYP basis set is adequate to calculate the energy levels of azomethine derivatives.[51] The similar trend of HOMO and LUMO energy levels contingent on structure for both experimental and calculated values confirms that the chosen theoretical method is suitable for predicting the properties of the compounds from Chart 1 that otherwise could not be prepared. The effect of the azomethine bond with the electron withdrawing groups (**2** versus **3**, **4** versus **5**, etc.), orientation of the heteroatomic bond (**11** versus **12**), and symmetry of the azomethines (**11** versus **13**) can also be accurately evaluated empirically.

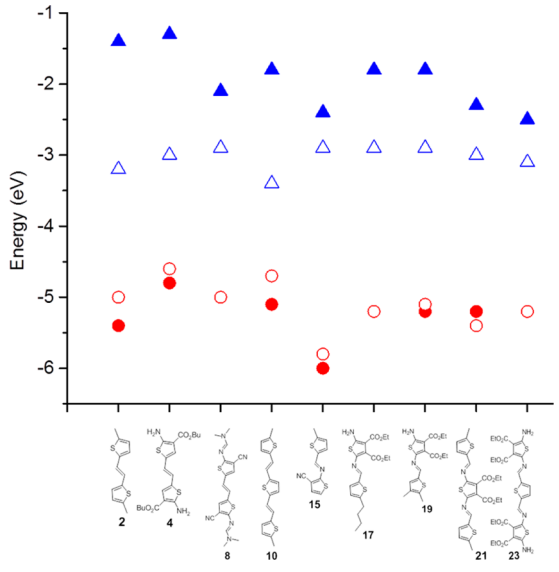

Figure 8. Comparison of experimental (open symbols) and calculated (filled symbols) HOMO (●) and LUMO (▲) in dichloromethane. The HOMO energy levels for **8**, **17**, and **23** were not included because the calculated and experimental values are identical.

The HOMO and LUMO energy levels of the compounds that could not be synthesized were subsequently calculated. The energy gap was additionally calculated from the difference between the HOMO and LUMO energy levels. The maximum absorbance was also calculated using time-dependent density functional theory of the first excited state. The properties were both analyzed in a vacuum and dichloromethane to assign solvent effects. This is particularly important because the energy levels, and hence the absorbance spectra of amine containing compounds such as **16**−**19**, **22**, and **23** are highly dependent on solvent polarity.[52,53] The combined calculated values are found in Table 3. The effect of the azomethine on the properties is evident from the collective theoretical calculations. For example, comparing **2** with its counterpart **3**, the HOMO and LUMO energy levels in both a vacuum and dichloromethane are lower for the azomethine. This leads to a bathochromic shift in the theoretical absorbance maximum. This is consistent with the experimental data. The HOMO and LUMO levels are further lower for **5** versus **4**, **15** versus **14**, **17** versus **16**, **19** versus **18**, **11**, **12**, and **13** versus **10**, **21** versus **20**, and **23** vs **22**. The HOMO energy level of **8** (−5.0 eV) is additionally lower than that of **9** (−4.8 eV). However, it has a 0.3 eV higher LUMO energy level owing to the electron withdrawing character of the azomethine. The contribution of the heteroatomic bond in **9** causes a blue shift (417 nm) in the absorbance spectra relative to its all-carbon counterpart (426 nm).

The effect of the withdrawing and donating groups on the energy levels can be seen by comparing the calculated values of **4**, **5**, **6**, and **7**. The electron withdrawing azomethine bond decreases the HOMO and LUMO energy values for **5** versus **4** and **7** versus **6**. This gives rise to a bathochromic shift for all the absorbance of the azomethine derivatives compared to their all-carbon counterparts. The electron withdrawing ester also stabilizes the HOMO and LUMO levels, resulting in a small bathochromic shift in the absorbance maximum. This also was observed when we compare **20** to **10**. The effect of the terminal amine on the properties can also be seen when we compare **2** versus **6** and **3** versus **7**. The electron donating group increases the HOMO and LUMO energy levels for both series. This leads to a bathochromic shift in the absorbance for the amine-terminated compounds, owing to the electronic *push*−*push* effect of the conjugated amine−azomethine groups.

The effect of the azomethine orientation can also be assessed by examining the calculated energy levels of **11**, **12**, and **13**. The data shows that the energy difference between the HOMO and LUMO energy values is consistent, regardless of the azomethine orientation. The orientation of the dipole moment created by the azomethine perturbs the HOMO energy levels by 0.2 eV. Similarly, the LUMO energy levels are perturbed by

dx.doi.org/10.1021/jo401497z | J. Org. Chem. 2013, 78, 9258−9269

Table 3. HOMO and LUMO Energy Levels, Energy Gaps, and Absorbance Maximum Theoretically Calculated by DFT B3LYP 6-31G* in Both a Vacuum and Dichloromethane

	vacuum				dichloromethane			
compound	HOMO (eV)	LUMO (eV)	E_g (eV)	λ_{abs} (nm)	HOMO (eV)	LUMO (eV)	E_g (eV)	λ_{abs} (nm)
2	−4.9	−1.3	3.6	331	−5.0	−1.4	3.6	332
3	−5.2	−1.7	3.5	338	−5.3	−1.8	3.5	340
4	−4.6	−1.2	3.4	355	−4.6	−1.3	3.3	364
5	−4.8	−1.5	3.3	370	−4.9	−1.7	3.2	380
6	−4.2	−0.9	3.3	352	−4.3	−1.1	3.2	359
7	−4.4	−1.3	3.1	364	−4.6	−1.5	3.1	372
8	−5.0	−2.1	2.9	426	−5.0	−2.1	2.9	426
9	−4.5	−1.5	3.0	417	−4.8	−1.8	3.0	417
10	−4.6	−1.7	2.9	415	−4.7	−1.8	2.9	416
11	−5.1	−2.3	2.8	423	−5.2	−2.4	2.8	424
12	−4.9	−2.0	2.9	416	−5.1	−2.2	2.9	414
13	−5.0	−2.1	2.9	429	−5.2	−2.3	2.9	421
14	−5.4	−1.9	3.5	344	−5.3	−2.0	3.3	359
15	−5.8	−2.4	3.4	347	−5.8	−2.4	3.4	347
16	−4.9	−1.4	3.5	352	−4.9	−1.5	3.4	356
17	−5.2	−1.8	3.4	361	−5.2	−1.8	3.4	367
18	−4.9	−1.3	3.6	343	−5.0	−1.4	3.6	350
19	−5.1	−1.7	3.4	356	−5.1	−1.8	3.3	361
20	−5.0	−1.7	3.3	396	−5.1	−1.8	3.3	400
21	−5.2	−2.0	3.2	416	−5.4	−2.3	3.1	422
22	−4.8	−1.9	2.9	434	−4.8	−1.9	2.9	443
23	−5.1	−2.3	2.8	469	−5.2	−2.5	2.7	487

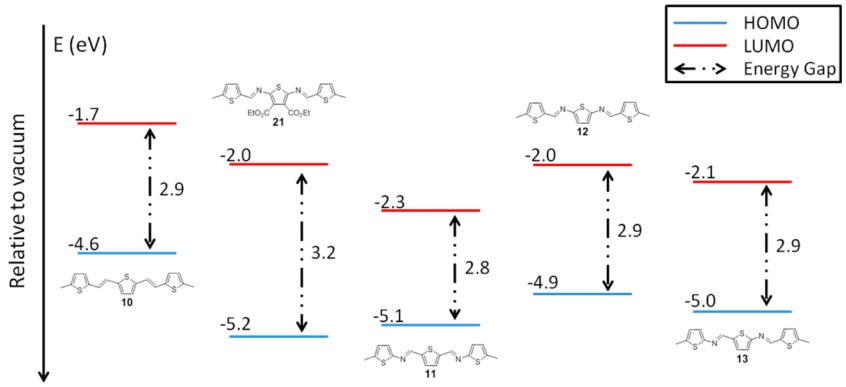

Figure 9. Calculated HOMO and LUMO energy levels for **10**, **11**, **12**, **13**, and **21** relative to vacuum.

0.3 eV. Lower energy values were found when the heteroatom was adjacent to the external thiophene (**11**). The calculated absorbance maxima were also consistent with the calculated energy gaps. The differences in the energy level are seen in Figure 9. This figure also clearly shows the effect of adding the azomethine linkages on the calculated HOMO energy level. Although the HOMO energy levels are lower, the energy gap is consistent because both the HOMO and LUMO energy levels are similarly perturbed.

The frontier orbitals were also investigated. Figure 10 shows an example for **4** and its analog **5**. It can be observed that, in both cases, the HOMO frontier orbitals are evenly distributed across the conjugated network. The same trend was also observed for the triads. In contrast, LUMO frontier orbitals are localized on the vinyl and azomethine bonds. This trend was similarly observed for all the dyads (see the Supporting Information). However, the LUMO was extended over the central thiophene and the conjugated bonds for the triads. This leads to intramolecular charge transfer of density over the entire molecule. This was previously observed with conjugated azomethine derivatives.[32] The vinyl and azomethine also show the same trend in terms of electron delocalization. Therefore, the DFT calculation clearly supports the fact that the azomethine and vinyl linkages are isoelectronic.

■ CONCLUSION

The photophysical and electrochemical properties of azomethines and their analogous all-carbon counterparts were analyzed. It was shown that it is possible to adjust the optoelectronic properties by incorporating different functional groups in the molecules. The vinyl compounds showed reversible oxidation in comparison to the azomethine, indicating that they are more stable under harsh conditions than their analogs. The collective spectral and electrochemical data revealed that the heteroatom had little effect on the properties of the conjugated dyads and triads. Only a 20 nm spectral red shift was observed between all-carbon and azomethine analogues. The only effect of the heteroatom was

dx.doi.org/10.1021/jo401497z | J. Org. Chem. 2013, 78, 9258−9269

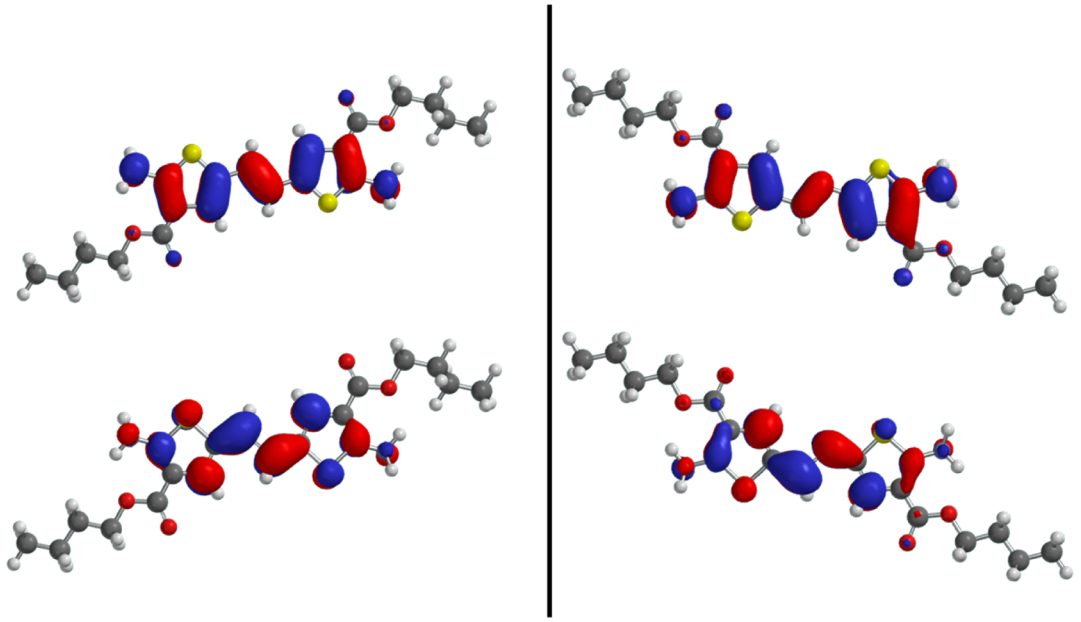

Figure 10. Calculated HOMO (top) and LUMO (bottom) frontier orbitals of **4** (left) and **5** (right) in dichloromethane.

for the fluorescence quantum yields. The azomethine fluorescence was not quenched by photoisomerization between the $E \rightarrow Z$ isomers, unlike its vinylene counterparts. The similar properties between the isoelectronic bonds were further confirmed by DFT studies. Taking into consideration the photochemical stability, greater ease of synthesis, and similar optoelectronic properties, azomethines are good alternatives to their all-carbon counterparts. Azomethines having potentially suitable properties for use in plastic devices, can therefore be designed on the basis of their all-carbon counterparts that have been successfully used as functional materials in working devices.

EXPERIMENTAL SECTION

General Procedures. All chemicals and reagents were obtained from commercial sources unless otherwise stated. Anhydrous and deaerated solvents were obtained from an activated alumina solvent purification system. $CDCl_3$ was repeatedly passed over a plug of activated basic alumina to remove undesired acid contaminants.

Spectroscopy. Absorbance measurements were done on a commercial UV−visible−NIR absorbance spectrophotometer and the fluorescence measurements were performed on UV−visible combined time-resolved and steady-state fluorometer after deaerating the samples with nitrogen for 20 min. The absolute quantum yields were measured using an integrating sphere.

Electrochemistry. Cyclic voltammetry measurements were made on a multichannel potentiostat. Compounds were dissolved in deaerated dichloromethane at 10^{-4} M with 0.5 M NBu_4PF_6. A platinum electrode was used as the working electrode with a platinum wire as the auxiliary electrode. The reference electrode was a silver wire. Ferrocene was added to the solution as an internal reference (E_{pa} = 0.435 V versus saturated calomel electrode (SCE)).[54]

Crystal Structure Determination. Suitable X-ray monocrystals of **8** were obtained by the slow evaporation of acetone (Table 4). X-ray diffraction measurements were performed on a diffractometer using graphite-monochromatized Cu Kα radiation with 1.541 78 Å. The structures were solved by direct methods (SHELXS97). All non-hydrogen atoms were refined based on FF_{obs}^2 (SHELXS97), whereas hydrogen atoms were refined on the calculated positions with fixed isotropic U, using riding model techniques.

Theoretical Calculations. Theoretical calculations were done with a commercially available software package.[55] The geometries were first optimized semi-empirically using AM1. These geometries were compared to the crystal structures of known compounds. Single point energies were then calculated from the optimized geometries using the DFT ab initio method with the B3LYP 6-31 G* basis set.

Table 4. Details of the Crystal Structure Determination of 8

formula	$C_{18}H_{18}N_6S_2$
mol wt (g/mol); F(000)	382.50 g/mol; 1600
cryst color and form	orange platelet
cryst size (mm)	0.18 × 0.06 × 0.04
T (K); d_{calcd} (g/cm^3)	150 (2); 1.363
cryst syst	orthorhombic
space group	*Pbca*
unit cell: a (Å)	16.0473 (6)
b (Å)	8.2489 (3)
c (Å)	28.1693 (11)
α (deg)	90.000
β (deg)	90.000
γ (deg)	90.000
V (Å^3); Z	3728.8 (2); 8
θ range (deg); completeness	3.14−72.54; 0.982
collected/independent reflections; R_{int}	49300/3680; 0.053
μ (mm^{-1}) abs. corr.	2.705 semiempirical
R1(F); wR (F^2) [$I > 2\sigma(I)$]	0.0541; 0.1413
R1(F); wR (F^2) (all data)	0.0651; 0.1467
GOF(F^2)	1.009
max. residual e$^-$ density	1.398 e$^-$·Å^{-3}

Synthesis. The synthesis of **10**, **21**, and **23** were done according to known methods.[24,25] All high-resolution mass spectrometry (HRMS) measurements were done in the electrospray ionization (ESI) mode with a time-of-flight (TOF) analyzer.

(E)-1,2-Bis(5-methylthiophen-2-yl)ethene (2). In a two-necked round-bottom flask, 5-methylthiophene-2-carbaldehyde (0.50 g, 1.4 mmol) was dissolved in anhydrous THF (8 mL). Titanium(IV) chloride (0.52 mL, 4.7 mmol) was then added dropwise at −18 °C, and the solution was stirred for 30 min. Zinc powder (0.62 g, 9.5 mmol) was added over a period of 30 min, and the reaction mixture was stirred for another 30 min at −18 °C. The reaction mixture was then refluxed for 3.5 h. After, the mixture was then poured into iced water. The organic layer was extracted with ethyl acetate. The product

dx.doi.org/10.1021/jo401497z | J. Org. Chem. 2013, 78, 9258−9269

was recrystallized in carbon tetrachloride, and it was washed with cold ethanol to afford the product as a yellow powder (453 mg, 52%). ^{1}H NMR ($CDCl_3$): δ = 6.83 (s, 1H), 6.78 (^dJ = 3.6 Hz, 1H), 6.62 (m, 1H), 2.47 (^dJ = 0.8 Hz, 3H). ^{13}C NMR ($CDCl_3$): δ = 141.0, 139.3, 126.3, 126.2, 121.1, 16.1. HRMS (ESI+): calcd for $C_{12}H_{13}S_2$ [M + H$^+$], 221.0453; found, 221.0450.

*Butyl 2-Cyanoacetate (**4a**).* Cyanoacetic acid (10 g, 117.5 mmol) was dissolved in *n*-butanol (10.9 mL, 117.5 mmol). Zinc perchlorate hexahydrate (21.9 g, 58.7 mmol) and magnesium sulfate (14.14 g, 117.5 mmol) were then added to the solution. The resulting slurry was stirred at 80 °C overnight. The reaction mixture was cooled to room temperature. The resulting precipitate was filtered, and it was washed with ethyl acetate. The organic extracts were concentrated, the residue was taken up into dichloromethane, and the solid was filtered. The filtrate was then washed with water and then with saturated $NaHCO_3$. After removing the solvent under a vacuum, we purified the crude product by silica gel flash column chromatography using hexane/ethyl acetate (90/10) as the eluent. The product was isolated as a colorless oil (12.73 g, 77%). ^{1}H NMR (acetone-d_6): δ = 4.18 (^tJ = 6.4 Hz, 2H), 3.79 (s, 2H), 1.67−1.60 (m, 2H), 1.45−1.35 (m, 2H), 0.94−0.90 (^tJ = 7.6 Hz, 3H). ^{13}C NMR (acetone-d_6): δ = 165.7, 115.8, 67.6, 32.1, 25.8, 20.5, 20.5, 14.8. HRMS (ESI+): calcd for $C_7H_{11}NO_2$ [M + Ag$^+$], 247.9835; found, 247.9837.

*Butyl 2-Aminothiophene-3-carboxylate (**4b**).* In a two-necked round-bottom flask, 4-dithiane-2,5-diol (0.54 g, 3.54 mmol), and **4a** (1 g, 7.08 mmol) were added. Anhydrous dimethylformamide (0.5 mL) was added followed by triethylamine (0.5 mL, 3.54 mmol) at 0 °C. The reaction mixture was then heated to 45 °C for 1.5 h. The reaction mixture was poured into ice water. The organic layer was extracted with dichloromethane, and it was then dried with magnesium sulfate. The salts were removed, and the organic layers were concentrated. The product was purified by silica gel flash chromatography with hexanes/ethyl acetate (70/30) to give the title compound as a yellow oil (0.41 g, 58%). ^{1}H NMR (acetone-d_6): δ = 6.93−6.91 (^dJ = 6.4 Hz, 1H), 6.87 (s, 1.4H), 4.21−4.18 (^tJ = 6.4 Hz, 2H), 1.70−1.63 (m, 2H), 1.47−1.38 (m, 2H), 0.96−0.92 (^tJ = 7.6 Hz, 3H).^{13}C NMR (acetone-d_6): δ = 166.7, 165.6, 127.2, 107.9, 107.3, 64.7, 32.6, 20.9, 15.0. HRMS (ESI+): calcd for $C_9H_{13}NO_2S$ [M + Ag+], 305.9712; found, 305.9699.

*Butyl 2-(((Trifluoromethoxy)carbonyl)amino)thiophene-3-carboxylate (**4c**).* In an oven-dried round-bottom flask, **4b** (1.15 g, 5.81 mmol) was dissolved in dichloromethane (5 mL). Trifluoroacetic anhydride (TFAA; 0.96 mL, 6.97 mmol) was added at 0 °C, followed by the dropwise addition of triethylamine (1 mL). The reaction mixture was stirred at room temperature overnight. It was then diluted in dichloromethane and washed with brine and water. The organic layer was dried over sodium sulfate, filtered, concentrated, and then purified by silica gel flash chromatography with hexanes/ethyl acetate (90/10). The title compound was isolated as a white solid (895 mg, 50%). ^{1}H NMR (acetone-d_6): δ = 12.00 (s, 1H), 7.31 (^dJ = 5.6 Hz, 1H), 7.19 (^dJ = 5.6 Hz, 1H), 4.38−4.35 (^tJ = 6.4 Hz, 2H), 1.79−1.76 (m, 2H), 1.51−1.47 (m, 2H), 1.01−0.98 (^tJ = 7.6 Hz, 3H). ^{13}C NMR (acetone-d_6): δ = 167.0, 155.0, 146.9, 126.0, 120.6, 118.1, 66.9, 32.3, 20.8, 15.0. HRMS (ESI+): calcd for [$C_{11}H_{12}F_3NO_3S$ + H]$^+$, 296.0569; found, 296.0555.

*Butyl 2-(((Trifluoromethoxy)carbonyl)amino)formylthiophene-3-carboxylate (**4d**).* In a dry two-necked flask, phosphorus oxychloride (0.13 mL, 1.44 mmol) was added to dimethylformamide (0.11 mL, 1.44 mmol) at 0 °C. **4c** (0.150 g, 0.48 mmol) diluted in tetrahydrofuran (5 mL) was then added. The reaction mixture was heated to 60 °C overnight, and then it was poured into ice water. The crude product was extracted with dichloromethane, dried with magnesium sulfate, filtered, and then concentrated. The product was purified by silica gel flash chromatography with hexanes/ethyl acetate (80/20) to afford the title compound as a white powder (116.6 mg, 72%). ^{1}H NMR (acetone-d_6): δ = 9.67 (s, 1H), 8.01 (s, 1H), 7.97, (s, 1H), 4.20−4.16 (^tJ = 6.4 Hz, 2H), 3.24 (s, 3H), 3.13 (s, 3H), 1.72−1.65 (m, 2H), 1.51−1.42 (m, 2H), 0.97−0.93 (^tJ = 7.2 Hz, 3H). ^{13}C NMR (acetone-d_6): δ = 183.7, 173.7, 164.3, 158.1, 142.4, 131.3, 119.8, 65.3, 41.7, 36.1, 32.6, 20.9, 15.0.

*(E)-Dibutyl 5,5′-(Ethene-1,2-diyl)bis(2-aminothiophene-3-carboxylate) (**4**).* In a two-necked flask, **2d** (0.20 g, 0.6 mmol) was dissolved in anhydrous THF (14 mL). Titanium(IV) chloride (0.32 mL, 2.4 mmol) was added dropwise at −18 °C, and the reaction mixture was stirred for 30 min. Zinc powder (0.44 g, 4.7 mmol) was added over a period of 30 min, and the slurry was stirred at the same temperature for another 30 min. The reaction mixture was then refluxed for 3.5 h. Afterward, the resulting solution was poured into ice water and the organic layer was extracted with ethyl acetate. The crude mixture was then poured into a solution of K_2CO_3 (0.5 g in 20 mL methanol and 4 mL water) and it was stirred for 3 h under nitrogen. The solvent was evaporated, and the crude product was extracted with ethyl acetate and concentrated under a vacuum. Purification of the crude mixture over silica gel flash chromatography (70/30, hexanes/ethyl acetate) gave **4** as a yellow powder (97 mg, 77%). ^{1}H NMR (acetone-d_6): δ = 7.17 (s, 1.6H), 6.87 (s, 1H), 6.52 (s, 1H), 4.2 (m, 2H), 1.70 (m, 2H), 1.47 (m, 2H), 0.97 (m, 3H). ^{13}C NMR (acetone-d_6): δ = 165.1, 163.3, 124.6, 123.7, 119.0, 105.7, 63.3, 31.2, 19.4, 13.5. HRMS (ESI+): calcd for $C_{20}H_{27}N_2O_4S_2$ [M + H$^+$], 423.14068; found, 423.1395.

*(E)-N′-(3-Cyano-5-formylthiophen-2-yl)-N,N-dimethylformimidamide (**8b**).* In an oven-dried two-necked flask, phosphorus oxychloride (12 mL, 128 mmol) was added dropwise at 0 °C in anhydrous dimethylformamide (40 mL, 516 mmol). The solution was stirred for 20 min, followed by the addition of **8a** (4 g, 32 mmol). The reaction mixture was stirred at room temperature for 40 min. The mixture was then heated at 50 °C overnight, and afterward the reaction mixture was poured into ice water and the crude product was extracted with ethyl acetate. The organic layer was further washed with water. The organic layers were combined, dried with magnesium sulfate, filtered, and then concentrated to give a yellow solid (3.5 g, 53%). ^{1}H NMR (acetone-d_6): δ = 9.78 (s, 1H), 8.20 (s, 1H), 7.94 (s, 1H), 3.32 (s, 1H), 3.20 (s, 1H). ^{13}C NMR (acetone-d_6): δ = 183.2, 175.6, 159.1, 140.6, 132.5, 116.4, 100.3, 42.2, 36.5. HRMS (ESI+): calcd for [$C_9H_9N_3OS$ + H] $^+$, 208.0539; found, 208.0534.

*(1E,1′E)-N′,N″-(5,5′-((E)-Ethene-1,2-diyl)bis(3-cyanothiophene-5,2-diyl))bis(N,N-dimethylformimidamide) (**8**).* In a two-necked round-bottom flask **8b** (0.50 g, 2.4 mmol) was dissolved in anhydrous THF (8 mL). Titanium(IV) chloride (0.82 mL, 8.1 mmol) was added dropwise at −18 °C, and the reaction mixture was stirred for 30 min. Zinc powder (1.1 g, 16.3 mmol) was added over a period of 30 min, and the slurry was stirred at the same temperature for another 30 min. The reaction mixture was then refluxed for 3.5 h. It was then poured into ice water and the organic layer was extracted with ethyl acetate. The product was purified by silica gel chromatography using ethyl acetate/hexane (20/80) to give the product as a yellow powder (0.53 g, 57%). ^{1}H NMR ($CDCl_3$): δ = 9.66 (s, 1H), 8.16 (s, 1H), 7.92 (s, 1H), 3.31 (s, 3H), 3.18 (s, 3H). ^{13}C NMR (acetone-d_6): δ = 165.8, 155.9, 130.4, 125.9, 120.6, 115.7, 97.5, 73.3, 72.3, 40.3. 34.6. HRMS (ESI+): calcd for $C_{18}H_{19}N_6S_2$ [M + H$^+$], 383.1107; found, 383.1090.

*(E)-2-((5-Methylthiophen-2-yl)methyleneamino)thiophene-3-carbonitrile (**15**).* In a round-bottom flask, 2-aminothiophene-3-carbonitrile (100 mg, 0.8 mmol) and 5-methylthiophene-2-carbaldehyde (67 mg, 0.53 mmol) were dissolved in anhydrous ethanol. A catalytic amount of trifluoroacetic acid (TFA) was added and the mixture was stirred overnight at room temperature. The resulting precipitate was filtered and it was washed with cold ethanol to give the title compound as a yellow powder (0.11 g, 88%). ^{1}H NMR (acetone-d_6): δ = 8.78 (s, 1H), 7.65 (^dJ = 3.6 Hz, 1H), 7.40 (^dJ = 5.6 Hz, 1H), 7.27 (^dJ = 5.6 Hz, 1H), 6.98 (^dJ = 2.8 Hz, 1H), 2.60 (s, 1H). ^{13}C NMR (acetone-d_6): δ = 165.2, 156.6, 151.1, 141.2, 138.4, 129.5, 129.3, 123.5, 116.1, 106.8, 17.0. HRMS (ESI+): calcd for $C_{11}H_9SN_2S$ [M + H$^+$], 233.0202; found, 233.0198.

*(E)-Diethyl 2-Amino-5-((5-butylthiophen-2-yl)methyleneamino)-thiophene-3,4-dicarboxylate (**17**).* Both 2, 5-diaminothiophene-3,4-dicarboxylic acid (77 mg, 0.3 mmol) and 5-butylthiophene-2-carboxaldehyde (50 mg, 0.3 mmol) were dissolved in ethanol (10 mL) before adding a catalytic amount of TFA (5 μL). The mixture was stirred at room temperature overnight and the organic layer was washed with water, and extracted with dichloromethane. After the solvent was removed under reduced pressure, the product was purified

dx.doi.org/10.1021/jo401497z | J. Org. Chem. 2013, 78, 9258−9269

by silica gel chromatography using dichloromethane and triethylamine (10%) as an eluent. The product was isolated as a yellow powder (0.02 g, 20%). ^{1}H NMR (acetone-d_6): δ = 8.17 (s, 1H), 7.45 (s, 2H), 7.34 (d, 1H, J = 3.6 Hz), 6.88 (d, 1H, J = 3.6 Hz), 4.33 (dd, 2H, J = 7.2 Hz), 4.21 (dd, 2H, J = 7.2 Hz), 2.87 (t, 6H, J = 8.8 Hz), 1.72 (m, 2H), 1.40−1.26 (m, 4H), 0.95 (t, 3H, J = 7.6 Hz). ^{13}C NMR (acetone-d_6): δ = 165.1, 164.4, 160.9, 151.7, 146.4, 140.8, 133.3, 132.5, 129.8, 126.0, 61.0, 59.9, 33.9, 22.3, 14.3, 14.1, 13.5. HRMS (ESI+): calcd for $C_{19}H_{24}N_2O_4S_2$ [M + H$^+$], 409.1250; found 409.1249.

*(E)-Diethyl 2-Amino-5-((4,5-dimethylthiophen-2-yl)-methyleneamino)thiophene-3,4-dicarboxylate (**19**).* Both 2,5-diaminothiophene-3,4-dicarboxylic acid (792 mg, 3.1 mmol) and 4,5-dimethylthiophene-2-carbaldehyde (430 mg, 3.1 mmol) were dissolved in ethanol (20 mL) before the addition of a catalytic amount of TFA (10 μL). The reaction mixture was stirred at room temperature overnight, washed with water, and extracted with dichloromethane. After the crude product was concentrated under a vacuum, the product was purified by silica gel chromatography using dichloromethane and triethylamine (10%) as the eluent. The title compound was isolated as a yellow powder (0.88 g, 75%). ^{1}H NMR ($CDCl_3$): δ = 7.93 (s, 1H), 7.03 (s, 1H), 6.25 (s, 2H), 4.39 (dd, 2H, J = 7.2 Hz), 4.22 (dd, 2H, J = 7.2 Hz), 2.35 (s, 3H),2.10 (s, 3H), 1.42 (t, 3H, J = 7.2 Hz), 1.29 (t, 3H, J = 7.2 Hz). ^{13}C NMR ($CDCl_3$): δ = 165.9, 164.9, 159.4, 146.7, 140.1, 137.9, 134.8, 134.7, 128.6, 61.9, 60.6, 14.9, 14.6, 14.3, 13.9. HRMS (ESI+): calcd for $C_{17}H_{20}N_2O_4S_2$ [M + H$^+$], 381.0937; found, 381.0943.

■ ASSOCIATED CONTENT

Supporting Information

^{1}H and ^{13}C NMR spectra of all compounds, UV−visible and fluorescence spectra, cyclic voltammograms, calculated HOMO and LUMO frontier orbitals, calculated atom coordinates, and absolute energies. A simplified chart of synthesized and synthetically unavailable compounds is also presented. This material is available free of charge via the Internet at http://pubs.acs.org.

■ AUTHOR INFORMATION

Corresponding Author

*W. G. Skene. E-mail: w.skene@umontreal.ca.

Notes

The authors declare no competing financial interest.

■ ACKNOWLEDGMENTS

Financial support from the Natural Sciences and Engineering Research Council of Canada is acknowledged for Discovery, Strategic Research, and Research Tools and Instrument grants. The Canadian Foundation for Innovation is also acknowledged for additional equipment and infrastructures. The Center for Self-Assembled Chemical Structures is also acknowledged. A.B. thanks NSERC, Fondation Québécoise pour la Recherche en Nature et Technologies and the Université de Montréal for graduate scholarships. Amélie Guérin is acknowledged for her help with preliminary cyclic voltammetry measurements.

■ REFERENCES

(1) Xue, S.; Yao, L.; Shen, F.; Gu, C.; Wu, H.; Ma, Y. *Adv. Funct. Mater.* **2012**, *22*, 1092.
(2) Guo, Y.; Yu, G.; Liu, Y. *Adv. Mater.* **2010**, *22*, 4427.
(3) Zhan, X.; Zhu, D. *Polym. Chem.* **2010**, *1*, 409.
(4) Beaujuge, P. M.; Reynolds, J. R. *Chem. Rev.* **2010**, *110*, 268.
(5) Schluter, A. D. *J. Polym. Sci., Part A: Polym. Chem.* **2001**, *39*, 1533.
(6) Das, S.; Pati, P. B.; Zade, S. S. *Macromolecules* **2012**, *45*, 5410.
(7) Wanfei, L.; Ming, Z.; Yang, L.; Qingquan, Z.; Zezhu, H.; Nakai Technology Company, Ltd., People's Republic of China, Organic copolymerized semiconductor material containing EDOT (3,4-ethylenedioxy thiophene)(3,4-ethylenedioxythiophene) electron donor cell. CN 102504208, June 20, 2012.
(8) Shin, R. Y. C.; Sonar, P.; Siew, P. S.; Chen, Z.-K.; Sellinger, A. *J. Org. Chem.* **2009**, *74*, 3293.
(9) Duan, C.; Huang, F.; Cao, Y. *J. Mater. Chem.* **2012**, *22*, 10416.
(10) Meier, H. *Angew. Chem., Int. Ed.* **2005**, *44*, 2482.
(11) Bolduc, A.; Mallet, C.; Skene, W. G. *Sci. China: Chem.* **2013**, *56*, 3.
(12) Bourgeaux, M.; Skene, W. G. *J. Org. Chem.* **2007**, *72*, 8882.
(13) Yang, C. J.; Jenekhe, S. A. *Chem. Mater.* **1991**, *3*, 878.
(14) Grigoras, M.; Antonoaia, N. C. *Polym. Int.* **2005**, *54*, 1641.
(15) Peeters, E.; van Hal, P. A.; Knol, J.; Brabec, C. J.; Sariciftci, N. S.; Hummelen, J. C.; Janssen, R. A. J. *J. Phys. Chem. B* **2000**, *104*, 10174.
(16) Subbiah, J.; So, F.; Reynolds, J. R.. US Patent 20,130,008,509, 2013.
(17) Lee, H.; Vak, D.; Baeg, K.-J.; Nah, Y.-C.; Kim, D.-Y.; Noh, Y.-Y. *J. Nanosci. Nanotechnol.* **2013**, *13*, 3321.
(18) Friend, R. H.; Gymer, R. W.; Holmes, A. B.; Burroughes, J. H.; Marks, R. N.; Taliani, C.; Bradley, D. D. C.; Dos Santos, D. A.; Bredas, J. L.; Lögdlund, M. *Nature* **1999**, *397*, 121.
(19) Sabnis, R. W.; Rangnekar, D. W.; Sonawane, N. D. *J. Heterocycl. Chem.* **1999**, *36*, 333.
(20) Puterova, Z.; Krutošíková, A.; Végh, D. *ARKIVOC* **2010**, *i*, 209.
(21) Buchstaller, H. P.; Siebert, C. D.; Lyssy, R. H.; Frank, I.; Duran, A.; Gottschlich, R.; Noe, C. R. *Monatsh. Chem.* **2001**, *132*, 279.
(22) Bartoli, G.; Boeglin, J.; Bosco, M.; Locatelli, M.; Massaccesi, M.; Melchiorre, P.; Sambri, L. *Adv. Synth. Catal.* **2005**, *347*, 33.
(23) Dong, Y.; Navarathne, D.; Bolduc, A.; McGregor, N.; Skene, W. G. *J. Org. Chem.* **2012**, *77*, 5429.
(24) Nakayama, J.; Fujimori, T. *Heterocycles* **1991**, *32*, 991.
(25) Dufresne, S.; Bolduc, A.; Skene, W. G. *J. Mater. Chem.* **2010**, *20*, 4861.
(26) Manecke, G.; Haertel, M. *Chem. Ber.* **1973**, *106*, 655.
(27) Dufresne, S.; Bourgeaux, M.; Skene, W. G. *J. Mater. Chem.* **2007**, *17*, 1166.
(28) Arunan, E.; Desiraju, G. R.; Klein, R. A.; Sadlej, J.; Scheiner, S.; Alkorta, I.; Clary, D. C.; Crabtree, R. H.; Dannenberg, J. J.; Hobza, P.; Kjaergaard, H. G.; Legon, A. C.; Mennucci, B.; Nesbitt, D. J. *Pure Appl. Chem.* **2011**, *83*, 1619.
(29) Janiak, C. *Dalton* **2000**, 3885.
(30) Dufresne, S.; Bolduc, A.; Skene, W. G. *Acta Crystallogr., Sect. E: Struct. Rep. Online* **2011**, *E67*, o3138.
(31) Dufresne, S.; Roche, I. U.; Skalski, T.; Skene, W. G. *J. Phys. Chem. C* **2010**, *114*, 13106.
(32) Dufresne, S.; Perez, G. S. A.; Bolduc, A.; Bourque, A. N.; Skene, W. G. *Photochem. Photobiol. Sci.* **2009**, *8*, 796.
(33) Guarin, S. A. P.; Bourgeaux, M.; Dufresne, S.; Skene, W. G. *J. Org. Chem.* **2007**, *72*, 2631.
(34) Seixas de Melo, J.; Elisei, F.; Gartner, C.; Aloisi, G. G.; Becker, R. S. *J. Phys. Chem. A* **2000**, *104*, 6907.
(35) Seixas de Melo, J.; Silva, L. M.; Arnaut, L. G.; Becker, R. S. *J. Chem. Phys.* **1999**, *111*, 5427.
(36) Becker, R. S.; Seixas de Melo, J.; Maçanita, A. L.; Elisei, F. *J. Phys. Chem.* **1996**, *100*, 18683.
(37) Turro, N. J.; Ramamurthy, V.; Scaiano, J. C. *Modern Molecular Photochemistry Of Organic Molecules*; University Science Books: Sausalito, CA, 2010.
(38) Tsang, D.; Bourgeaux, M.; Skene, W. G. *J. Photochem. Photobiol., A* **2007**, *192*, 122.
(39) Bard, A. J.; Faulkner, L. R. *Electrochemical Methods: Fundamentals and Applications*; 2nd ed.; John Wiley & Sons: New York, 2001.
(40) *Handbook of Electrochemistry*; Zoski, C. A., Ed.; Elsevier Science: Amsterdam, 2007.
(41) Sioda, R. E.; Frankowska, B. *J. Electroanal. Chem.* **2008**, *612*, 147.
(42) Page, J. A.; Wilkinson, G. *J. Am. Chem. Soc.* **1952**, *74*, 6149.
(43) Roncali, J. *Chem. Rev.* **1992**, *92*, 711.

(44) Pommerehne, J.; Vestweber, H.; Guss, W.; Mahrt, R. F.; Bässler, H.; Porsch, M.; Daub, J. *Adv. Mater.* **1995**, *7*, 551.
(45) Koepp, H. M.; Wendt, H.; Stkehlow, H. *Z. Elektrochem.* **1960**, *64*, 483.
(46) Sun, Q.; Wang, H.; Yang, C.; Li, Y. *J. Mater. Chem.* **2003**, *13*, 800.
(47) Lu, Y. Z.; Xiao, Z. G.; Yuan, Y. B.; Wu, H. M.; An, Z. W.; Hou, Y. B.; Gao, C.; Huang, J. S. *J. Mater. Chem. C* **2013**, *1*, 630.
(48) Connelly, N. G.; Geiger, W. E. *Chem. Rev.* **1996**, *96*, 877.
(49) Pastore, M.; Fantacci, S.; De, A. F. *J. Phys. Chem. C* **2010**, *114*, 22742.
(50) McCormick, T. M.; Bridges, C. R.; Carrera, E. I.; DiCarmine, P. M.; Gibson, G. L.; Hollinger, J.; Kozycz, L. M.; Seferos, D. S. *Macromolecules* **2013**, *46*, 3879.
(51) Sahu, H.; Panda, A. N. *Macromolecules* **2013**, *46*, 844.
(52) Bolduc, A.; Dong, Y.; Guerin, A.; Skene, W. G. *Phys. Chem. Chem. Phys.* **2012**, *14*, 6946.
(53) Mallet, C.; Le Borgne, M.; Starck, M.; Skene, W. G. *Polym. Chem.* **2013**, *4*, 250.
(54) Tsierkezos, N. *J. Solution Chem.* **2007**, *36*, 289.
(55) *Spartan*, 10 ed.; Wavefunction, Inc.: Irvine, CA, 2012.